Accepted Manuscript

Energetics of silica lithiation and its applications to lithium ion batteries

G. Lener, M. Otero, D.E. Barraco, E.P.M. Leiva
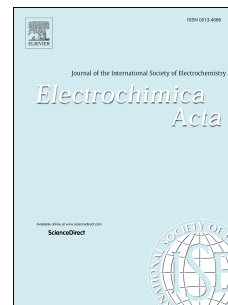
Energetics of silica lithiation and its applications to lithium ion batteries.

G. Lener,[1] M. Otero[1,2] D. E. Barraco,[1] E. P. M. Leiva[2]

[1] *IFEG-CONICET. Facultad de Matemática Astronomía y Física. Universidad Nacional de Córdoba. Argentina.*

[2] *INFIQC-CONICET. Departamento de Química Teórica y Computacional. Facultad de Ciencias Químicas. Universidad Nacional de Córdoba. Argentina.*

*Corresponding author: Ezequiel Leiva (*eze_leiva@yahoo.com.ar)

Abstract

Silica based materials are important candidates as anodes for lithium ion batteries due to their high specific capacity, low production and material cost and abundance in the earth crust. Silica lithiation leads to reversible and irreversible reactions to produce silicon, lithium oxide and lithium silicates. The final composition of these products confers a variety of electrochemical performances, particularly concerning their specific capacity and stability/cyclability of the electrodes. Knowledge on the thermochemistry of these reactions is relevant to analyze the thermodynamic stability and potential occurrence of the different phases. In this work, the free energy of reaction for the lithiation of silica is calculated for different products. The

present first principles studies indicate that the formation of products is a highly exothermic and endergonic process in all cases. In the case of SiO_2 lithiation, the free energy shows that the reaction to form $Li_2Si_2O_5$ is highly exothermic, having the greatest probability of formation. The lithiation potentials and stability of different products are analyzed in the context of experimental results from the literature.

Keywords: SiO_2 electrode; lithiation potential; free energy; DFT, lithium battery.

1. Introduction

Most commercialized lithium ion batteries (LIB) use graphite as anode material and this type of anodes is also being used in batteries that employ sulphur cathodes. [1–4]. A wide range of materials have been studied to replace graphite and to increase the capacity of the anodes [5]. The most promising materials are based on silicon, due to its high theoretical specific capacity, of 3579 mAh g^{-1}[6]. The main problem arises from the huge volume expansion of ~300% during silicon lithiation that produces a pulverization of the electrode and consequently the loss of electric contact [7]. Also, the prime silicon source in earth´s crust is crystalline silica SiO_2 (quartz), and to obtain pure grade silicon, a thermal or chemical reduction is necessary. The latter is an activated and expensive process. Industrially, silicon is usually obtained by reaction of silica and coal at 1500-2000 ℃ in arc electrode furnace. The enthalpy of the re action between quartz-SiO_2 and C to form Si and CO_2 is +4.49 eV [8], indicating that the process is very

endothermic. Other similar strategy is the reaction with iron at 2000 ℃ to form silicon and iron oxide. This reaction has an enthalpy of +5.50 eV [8], showing to be also a high endothermic process. Moreover, the most promising strategy to mitigate the huge volumetric change of the electrode in the lithiation/delithiation process is to use nano-structurated silicon [5,9,10] or silicon compounds, which makes the manufacturing process even more expensive.

As a more economical and environmentally friendly alternative, Chang et al. [11] proposed the use of quartz-SiO_2 as anode for LIB. To this end, the authors milled quartz-SiO_2 per 24 h to obtain amorphous SiO_2, reaching a stable specific capacity of 800 mAh g^{-1} over 200 cycles. The authors proposed that the milling process provides the formation of vacancies in SiO_2 species, thus increasing the reactivity towards lithiation. The authors determined the formation of Li_4SiO_4 and $Li_2Si_2O_5$ as products of lithiation in the first cycles, being irreversible and reversible processes respectively. Previously, Kim et al. employed Nuclear Magnetic Resonance (NMR) to study the formed species in the lithiation of SiO electrodes and determined the formation of Li_2O, Li_4SiO_4 and others lithium silicates[12]. Guo et al. studied the electrochemical reduction of a nano-SiO_2-hard carbon composite prepared by hydrothermal reaction [13]. The authors showed a high specific reversible capacity of 630 mAh g^{-1} and a good cyclability. Using the NMR technique they also determined the presence of Li_2O, Li_4SiO_4 and others forms of lithium silicates. Likewise, Sun et al., studied the reversible formation of $Li_2Si_2O_5$ in the lithiation of SiO thin film electrodes using the electron diffraction technique[14]. Maghrabi et al. presented a combinatorial studies of $Si_{x-1}O_x$ as a negative electrode for LIB [15].

The authors indicated that the amount of oxide phases should be optimized in order to obtain electrodes with desired specific reversible capacity and appropriate irreversible capacity. The formation of Li_2O and Li_4SiO_4 inactive phases helps to buffer volume expansion. Also, Nguyen et al. studied the role of oxygen composition in SiO_x electrodes preparing several materials with different stoichiometries [16]. The authors determined that higher oxygen contents increase the cyclability and the formation of Li_2O. On the other hand, it was shown that lithium silicates (Li_4SiO_4, Li_2SiO_3 and $Li_2Si_2O_5$) protect the electrode surface from the attack of the electrolyte. Moreover, the presence of siloxane groups on the SiO_x surface plays a crucial role in the immunity of the electrode surface, allowing the formation of a stable solid electrolyte interphase (SEI) [16] .

Beside of the previously described research, there are many investigations about the lithiation of SiO_x anodes in LIB, supporting the idea that the formation of products from reversible/irreversible reactions such as Li_2O, Li_4SiO_4, Li_2SiO_3 and $Li_2Si_2O_5$ is crucial. This is important to mitigate the volume expansion in the lithiation/delithiation process and to form a stable SEI layer, which avoids the attack of the electrolyte to the electrode [12,15–18]. Moreover, even silicon nanoparticles are surrounded with a thin shell of SiO_x, so that in the lithiation process the irreversible formation of Li_2O and lithium silicates also would occur [19].

The aim of the present work is to investigate the thermodynamics of SiO_2 lithiation and the stability of the formed products through different alternative reactions, such as Li_2O and lithium silicates, in the context of experimental results from the

literature. This was carried out by means of Density Functional Theory calculations (DFT) in the pseudopotential framework. To make an accurate description of the free energy of the system we take into account the electronic energy, calculated by DFT, and include the vibrational energy using perturbation theory, to include phonons contributions. Free energies, vibrational energies, density of states and lithiation potentials are analyzed in comparison with experimental data from bibliography.

2. Theory and calculation details

Density Functional Theory (DFT) calculations where performed using the Quantum Espresso package [20] with Vanderbilt ultrasoft pseudopotentials and the PBE exchange-correlation functional [21]. The Kohn-Sham orbitals and charge density were expanded in plane-waves basis set up to 750 and 6800 eV, respectively. The Brillouin zone was sampled with a Methfessel-Paxton [22] first-order method in a 8x8x8 irreducible Monkhorst-Pach k-point grid [23] and a 0.4 eV spreading. The convergence threshold for the total energy at each electronic calculation was set to 1.10^{-6} eV. The optimization of the cell parameters and the atomic positions were done using Broyden-Fletcher-Goldfarb-Shanno (BFGS) algorithm. The crystallographic structures to start the minimization procedure were taken from materials project repositories [8]. The crystallographic parameters of the relaxed structures are summarized in Table I. The free energy of reaction was obtained from electronic and phonon calculations as described below.

The change of Gibbs free energy for a given reaction is:

$$\Delta G = \Delta H - T\Delta S \qquad (1),$$

Where T is the absolute temperature, ΔS the entropy variation and ΔH the enthalpy variation according to:

$$\Delta H = \Delta U + p\Delta V + v\Delta P \qquad (2),$$

In the reactions studied in this work, the term correspondent to $p\Delta V$ is of the order of 10^{-7} eV, and will be neglected here. For the case of a system at constant pressure $\Delta P = 0)$, so that in the present calculations we approximate the enthalpy change by the internal energy change ($\Delta H \cong \Delta U$). So we have:

$$\Delta G \cong \Delta U - T\Delta S = \Delta F \qquad (3),$$

Where ΔF is the Helmholtz free energy change of the reaction, which has two contributions:

$$\Delta F = \Delta E_{DFT} + \Delta F_{vib} \qquad (4).$$

Where ΔE_{DFT} is the internal electronic energy (including electron-electron and electron-ion interactions) and ΔF_{vib} is the total vibrational free energy change. The latter can be calculated by the sum of the zero point internal energy changes

and the integration of the phonon density of states as function of the frequency of vibration according to:

$$\Delta F_{vib} = -\frac{\hbar}{2}\sum_i \omega_i + \kappa_B T \sum_i \ln\left(\frac{\hbar\omega_i}{\kappa_B T}\right) \quad (5)$$

where the sum runs over products and reactants.

Also, since the solids do not have translational and rotational movement, ΔS can be obtained directly from the vibrational energy as $\Delta S = -\partial \Delta F_{vib}/\partial T$. The lithiation potentials V where calculated as $V = -\frac{\Delta G}{n}$, were G is the free energy and n=1 is the amount of electrons involved in the lithiation reaction [24,25]. Since experimental V values are reported in the Li/Li$^+$ scale, bcc metallic lithium was used as standard state for the present free energy calculations.
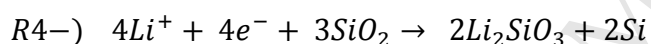
3. Result and Discussion

As mentioned above, several investigations using SiO_2 as negative electrode for LIB suggest the formation of silicon by electrochemical reduction of silica and the formation of Li_2O and different lithium silicates as co-products [9,11,13–15,26–28]. Moreover, the oxygen content in SiO_x must be optimized to favor irreversible reactions and the formation of products that mitigate the volume expansion/contraction in the lithiation/delithiation process [12,19,29]. Furthermore, it has been found in the literature [30–32] that oxygen content on the surface of the active material is also important for fabrication of electrodes due to its interaction

with the binder material [30,31], either due to the formation of esther like covalent bonds or hydrogen bonds [32]

According to the literature discussed in Section 1, the electrochemical reactions that may take place during the lithiation of SiO_2 can be summarized as:

$R1-)$ $\quad 4Li^+ + 4e^- + SiO_2 \rightarrow 2Li_2O + Si$

$R2-)$ $\quad 4Li^+ + 4e^- + 2SiO_2 \rightarrow Li_4SiO_4 + Si$

$R3-)$ $\quad 4Li^+ + 4e^- + 5SiO_2 \leftrightarrow 2Li_2Si_2O_5 + Si$

$R4-)$ $\quad 4Li^+ + 4e^- + 3SiO_2 \rightarrow 2Li_2SiO_3 + 2Si$
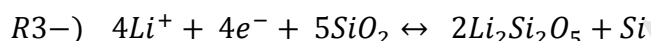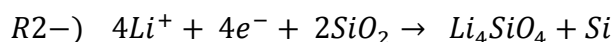
Considering that in reactions 1, 2 and 4 only the formed silicon will reversibly store lithium, and taking into account the specific theoretical capacity of $Li_{15}Si_4$, the theoretical specific capacities for the different reactions were calculated and are listed in Table II. For reaction 3, it must be considered that $Li_2Si_2O_5$ has been proposed to present reversible lithium storage, at a higher potential than that of Si. The coexistence of both reactions has been experimentally observed [14,33–35]. In this case, the theoretical specific capacity was calculated taking into account the reversible reaction to get $Li_2Si_2O_5$ and the reversible formation of $Li_{15}Si_4$ alloy. In the general case, where all the reactions written above may occur, the capacity will depend on the amounts and types of inactive phases formed in the reaction. Thus,

the measured capacity will be a function of the relative contributions of the different reactions, whose relative weight may present thermodynamic or kinetic control. In all cases the specific capacities are relatively high as compared with that of graphite (table II).

In thermochemical terms, the calculated ΔH values for reactions 1-4 (Table II) indicate that all reactions are highly exothermic. These results are in good agreement with previously reported theoretical and experimental values[8]. Although the reactions are highly exothermic, their spontaneity could be dependent of the entropy term. Therefore, the calculation of this term is important to obtain a complete analysis of the reactions. We obtain the vibrational contribution using phonon calculations as described above. The vibrational free energy contributions are shown in Figure 1.

Figure 1a shows the change in the vibrational free energy for the lithiation of SiO_2 as a function of temperature for the different reactions. All ΔF_{vib} are positive, indicating that the reactions are not favored by the vibrational contributions. Reaction 1 is the one that has the lowest ΔF_{vib}. Figure 1-b indicates that in all cases the vibrational entropy changes are negative and that the differences between the reactions are in the order of mili-eVs. Therefore, the spontaneity of the reactions will be dominated by the electronic internal energy difference (ΔE_{DFT}).

The different free energies of reaction as a function of temperature are shown in Figure 2-a. At room temperature, the free energy change of reactions 1-4 are -2.75, -4.78, -5.22, -5.03 eV respectively (Table II). These values denote high

exergonic reactions and the fact that the lithiation of SiO_2 to get $Li_2Si_2O_5$ is the thermodynamically most probable reaction at room temperature. This reaction was reported as reversible by Sun et al.[14]. The formation of Li_4SiO_4, observed in almost all experiments, is also favored thermodynamically.

The theoretical potentials of formation of different products are shown in Figure 2-b as a function of temperature. At room temperature, it is found that the formation of $Li_2Si_2O_5$ is the species favored at the higher potentials, above 1.3 V, while the occurrence of Li_2O becomes only be possible below 0.68 V. A wide range of values of formation potentials for the products of reactions 1-4 is reported in the literature (Table III) [12–14,33–37]. It is well known that the experimental formation potential depends on various factors, being mainly affected by the kinetics of lithium insertion [5]. This could make the experimental potentials to be lower than the values predicted by thermodynamics. In fact, Table III shows experimental lithiation potential values (column 2) for the formation of products (column 1) obtained upon SiO_2 lithiation. Different values are reported for the same product, depending on the different synthesis method used for silica. These results show that the nature of lithiation, the diffusional process and kinetics of the reaction depend on the nature of the SiO_2 employed. In fact, Ostadhossein et al. [38], using atomistic calculations, demonstrated the anisotropic transport of lithium into crystalline SiO_2 and the fact that the activation energy varies with the Li/O ratio in the pathway of diffusion. Thus, the present predictions of the lithiation potential of crystalline SiO_2 have to be used as a superior quote of the experimental value. It is remarkable that Li et al. show a cyclic voltammogram with peaks at 1.29 and 0.71 V, attributed to the

decomposition of solvent and formation of SEI layer [35] that are coincident with the present calculated lithiation potentials that could lead to Li_2SiO_3, $Li_2Si_2O_5$ and Li_2O, respectively. Moreover, several of the references listed in Table III show peaks around of 0.7 V, which is coincident with the lithiation potential corresponding to the formation Li_2O calculated here. It is also remarkable the occurrence of peaks close to 1.28 and 1.32 V, which would correspond to the formation of Li_2SiO_3 and $Li_2Si_2O_5$, see Figure 2b.

In the work of Jiao et al. [8], an anodic peak at 1.2 V was attributed to the reversible delithiation of $Li_2Si_2O_5$, but in the lithiation process the potential assigned to the formation of $Li_2Si_2O_5$ was 0.28 V. The difference between the cathodic and anodic peaks for the same process would indicate that the reaction is controlled by kinetics. Thus, the lower potentials measured experimentally could be attributed to kinetic limitations. Also, the initial amorphous structure of SiO_2 could cause all silicates to be formed at lower potentials than those predicted, yielding a wide voltammetric peak.

As mentioned above, the stability of the different products it also of practical importance, because they contribute to SEI formation, and will buffer the volume expansion of silicon during the lithiation/delithiation process. Figure 3-a shows the phonon density of states of the different products formed in the lithiation of SiO_2. It can be seen that the silicates present states at frequencies in the region between 800 and 1100 cm^{-1}. On the opposite, Li_2O does not present vibrational states in this region . Figure 3-b shows the electronic density of states of the different products formed in the lithiation of SiO_2. It can be seen that the silicates have electronics

states at more negatives values (with respect to the Fermi level) than Li_2O. The projected density of states indicates lower electronic occupations on the lithium atom for the case of silicates than in the case of the lithium oxide. Lithium silicates present more energetic electronic states than Li_2O due to the SiO_4^{4-} covalent and electronegative groups. A Mulliken population analysis [39], listed in Table II, indicates that in Li_2O the Li-O bond electrons are more localized on the Li atoms than in silicates, whereby Li_2O could result more reactive towards further reactions and could change the structure of the SEI. Thus, electronic analysis suggest that lithium silicates are more stable products than Li_2O. The present results bear also consequences for Li storage in Si nanostructures. In these cases, the surface of the nanostructures may be covered by an oxidized layer, where the present reactions could take place upon formation of the SEI. Thus, it can be stated that the lithium silicates may provide an additional stability to the SEI formed under these conditions, improving electrode cycling performance. On the other hand, special care should be taken in the present systems to prevent the occurrence of HF in $LiPF_6$ containing electrolytes (which could appear in the presence of small traces of water), since SiO_2 is known to be unstable in the presence of HF[40].

4. Conclusions

The energetics of the reactions taking place in the lithiation of silica to get silicon and different co-products was analyzed using first-principles calculations, yielding the related thermodynamics properties.

The results indicate that the reactions are all exothermic and exergonic, being the formation of $Li_2Si_2O_5$ and Li_2SiO_3 the most probable at higher potentials. The potential of lithiation calculated provides a way to understand the presence of different products found in experiment. The calculated values provide an upper bound which could be shifted experimentally towards lower potentials during the charge, depending on the kinetics of lithiation. Electronic structure analysis of the formed products suggest a major stability of lithium silicates with respect to lithium oxide. These products could provide an additional stability to the solid electrolyte interphase formed on silicon nanostructures.

Thus, knowledge of the thermodynamic properties as function of temperature may provide an important tool to optimize the experimental parameters to get desired active/inactive phases. This will result in the improvement of the cyclability and stability of the cell for different applications, using a low cost and abundant material as anode for lithium-ion batteries.

5. Acknowledgments

6. **References**.

[1]   A. Bhargav, M. Wu, Y. Fu, A Graphite-Polysulfide Full Cell with DME-Based Electrolyte, J. Electrochem. Soc. 163 (2016) A1543–A1549. doi:10.1149/2.0151608jes.

[2]   F. Xu, X. Li, F. Xiao, S. Xu, X. Zhang, P. He, H. Zhou, A battery with sulphur cathode and lithiated graphite anode based on Lithium shuttle reaction, Mater. Technol. 7857 (2016) 1–4. doi:10.1080/10667857.2016.1196564.

[3]   J. Balach, T. Jaumann, L. Giebeler, Nanosized Li2S-based cathodes derived from MoS2 for high-energy density Li–S cells and Si–Li2S full cells in carbonate-based electrolyte, Energy Storage Mater. (2017) 1–8. doi:10.1016/j.ensm.2017.03.013.

[4]   M. Piwko, T. Kuntze, S. Winkler, S. Straach, P. Härtel, H. Althues, S. Kaskel, Hierarchical columnar silicon anode structures for high energy density lithium sulfur batteries, J. Power Sources. 351 (2017) 183–191. doi:10.1016/j.jpowsour.2017.03.080.

[5]   M.N. Obrovac, V.L. Chevrier, Alloy negative electrodes for Li-ion batteries, Chem. Rev. 114 (2014) 11444–11502. doi:10.1021/cr500207g.

[6]   M.N. Obrovac, L. Christensen, Structural Changes in Silicon Anodes during Lithium Insertion/Extraction, Electrochem. Solid-State Lett. 7 (2004) A93–A96.

doi:10.1149/1.1652421.

[7]   X. Su, Q. Wu, J. Li, X. Xiao, A. Lott, W. Lu, B.W. Sheldon, J. Wu, Silicon-Based

Nanomaterials for Lithium-Ion Batteries: A Review, Adv. Energy Mater. 4 (2013) 1–

23. doi:10.1002/aenm.201300882.

[8]   A. Jain, S.P. Ong, G. Hautier, W. Chen, W.D. Richards, S. Dacek, S. Cholia, D.

Gunter, D. Skinner, G. Ceder, K.A. Persson, Commentary: The materials project: A

materials genome approach to accelerating materials innovation, APL Mater. 1

(2013). doi:10.1063/1.4812323.

[9]   M. Yoshio, H. Wang, K. Fukuda, T. Umeno, N. Dimov, Z. Ogumi, Carbon-Coated Si

as a Lithium-Ion Battery Anode Material, J. Electrochem. Soc. 149 (2002) A1598.

doi:10.1149/1.1518988.

[10]   B. Liang, Y. Liu, Y. Xu, Silicon-based materials as high capacity anodes for next

generation lithium ion batteries, J. Power Sources. 267 (2014) 469–490.

doi:10.1016/j.jpowsour.2014.05.096.

[11]   W.-S. Chang, C.-M. Park, J.-H. Kim, Y.-U. Kim, G. Jeong, H.-J. Sohn, Quartz

(SiO2): a new energy storage anode material for Li-ion batteries, Energy Environ.

Sci. 5 (2012) 6895. doi:10.1039/c2ee00003b.

[12]   T. Kim, S. Park, S.M. Oh, Solid-State NMR and Electrochemical Dilatometry Study

on Li+ Uptake/Extraction Mechanism in SiO Electrode, J. Electrochem. Soc. 154

(2007) A1112. doi:10.1149/1.2790282.

[13]   B. Guo, J. Shu, Z. Wang, H. Yang, L. Shi, Y. Liu, L. Chen, Electrochemical

reduction of nano-SiO2 in hard carbon as anode material for lithium ion batteries,

Electrochem. Commun. 10 (2008) 1876–1878. doi:10.1016/j.elecom.2008.09.032.

[14]   Q. Sun, B. Zhang, Z.-W. Fu, Lithium electrochemistry of SiO2 thin film electrode for

lithium-ion batteries, Appl. Surf. Sci. 254 (2008) 3774–3779.

doi:10.1016/j.apsusc.2007.11.058.

[15]   M. a. Al-Maghrabi, J. Suzuki, R.J. Sanderson, V.L. Chevrier, R. a. Dunlap, J.R. Dahn, Combinatorial Studies of Si1−xOx as a Potential Negative Electrode Material for Li-Ion Battery Applications, J. Electrochem. Soc. 160 (2013) A1587–A1593. doi:10.1149/2.115309jes.

[16]   C.C. Nguyen, H. Choi, S.-W. Song, Roles of Oxygen and Interfacial Stabilization in Enhancing the Cycling Ability of Silicon Oxide Anodes for Rechargeable Lithium Batteries, J. Electrochem. Soc. 160 (2013) A906--A914. doi:10.1149/2.118306jes.

[17]   M. Oschatz, J.T. Lee, H. Kim, W. Nickel, L. Borchardt, W.I. Cho, C. Ziegler, S. Kaskel, G. Yushin, Micro- and mesoporous carbide-derived carbon prepared by a sacrificial template method in high performance lithium sulfur battery cathodes, J. Mater. Chem. A. 2 (2014) 17649–17654. doi:10.1039/C4TA03327B.

[18]   J.Y. Kim, D.T. Nguyen, J.S. Kang, S.W. Song, Facile synthesis and stable cycling ability of hollow submicron silicon oxide-carbon composite anode material for Li-ion battery, J. Alloys Compd. 633 (2015) 92–96. doi:10.1016/j.jallcom.2015.01.309.

[19]   B. Philippe, R. Dedryvère, J. Allouche, F. Lindgren, M. Gorgoi, H. Rensmo, D. Gonbeau, K. Edström, Nanosilicon electrodes for lithium-ion batteries: Interfacial mechanisms studied by hard and soft X-ray photoelectron spectroscopy, Chem. Mater. 24 (2012) 1107–1115. doi:10.1021/cm2034195.

[20]   P. Giannozzi, S. Baroni, N. Bonini, M. Calandra, R. Car, C. Cavazzoni, D. Ceresoli, G.L. Chiarotti, M. Cococcioni, I. Dabo, A.D. Corso, S. De Gironcoli, S. Fabris, G. Fratesi, R. Gebauer, U. Gerstmann, C. Gougoussis, A. Kokalj, M. Lazzeri, L. Martin-samos, N. Marzari, F. Mauri, R. Mazzarello, S. Paolini, A. Pasquarello, L. Paulatto, C. Sbraccia, A. Smogunov, P. Umari, QUANTUM ESPRESSO: a modular and open-source software project for quantum simulations of materials, J. Phys. Condens. MATTER. 21 (2009) 1–19. doi:10.1088/0953-8984/21/39/395502.

[21]   J.P. Perdew, K. Burke, M. Ernzerhof, Generalized Gradient Approximation Made

Simple, Phys. Rev. Lett. 77 (1996) 3865–3868. doi:10.1103/PhysRevLett.77.3865.

[22]   M. Methfessel, A.T. Paxton, High-precision sampling for Brillouin-zone integration in metals, Phys. Rev. B. 40 (1989) 3616–3621. doi:10.1103/PhysRevB.40.3616.

[23]   H.J. Monkhorst, J.D. Pack, Special points for Brillouin-zone integrations, Phys. Rev. B. 13 (1976) 5188–5192. doi:10.1103/PhysRevB.13.5188.

[24]   A. Urban, D.-H. Seo, G. Ceder, Computational understanding of Li-ion batteries, Npj Comput. Mater. 2 (2016) 16002. doi:10.1038/npjcompumats.2016.2.

[25]   A. Jain, Y. Shin, K.A. Persson, Computational predictions of energy materials using density functional theory, Nat. Rev. Mater. 1 (2016) 15004. doi:10.1038/natrevmats.2015.4.

[26]   R. Zhang, Y. Du, D. Li, D. Shen, J. Yang, Z. Guo, H.K. Liu, A.A. Elzatahry, D. Zhao, Highly reversible and large lithium storage in mesoporous Si/C nanocomposite anodes with silicon nanoparticles embedded in a carbon framework, Adv. Mater. 26 (2014) 6749–6755. doi:10.1002/adma.201402813.

[27]   Z. Favors, W. Wang, H.H. Bay, A. George, M. Ozkan, C.S. Ozkan, Stable cycling of SiO2 nanotubes as high-performance anodes for lithium-ion batteries., Sci. Rep. 4 (2014) 4605. doi:10.1038/srep04605.

[28]   K. Yasuda, Y. Kashitani, S. Kizaki, K. Takeshita, T. Fujita, S. Shimosaki, Thermodynamic analysis and effect of crystallinity for silicon monoxide negative electrode for lithium ion batteries, J. Power Sources. 329 (2016) 462–472. doi:10.1016/j.jpowsour.2016.08.110.

[29]   D.J. Lee, H. Lee, M.H. Ryou, G.B. Han, J.N. Lee, J. Song, J. Choi, K.Y. Cho, Y.M. Lee, J.K. Park, Electrospun three-dimensional mesoporous silicon nanofibers as an anode material for high-performance lithium secondary batteries, ACS Appl. Mater. Interfaces. 5 (2013) 12005–12010. doi:10.1021/am403798a.

[30]   N.S. Hochgatterer, M.R. Schweiger, S. Koller, P.R. Raimann, T. Wöhrle, C. Wurm,

M. Winter, Silicon/Graphite Composite Electrodes for High-Capacity Anodes: Influence of Binder Chemistry on Cycling Stability, Electrochem. Solid-State Lett. 11 (2008) A76. doi:10.1149/1.2888173.

[31] D. Mazouzi, B. Lestriez, L. Roué, D. Guyomard, Silicon Composite Electrode with High Capacity and Long Cycle Life, Electrochem. Solid-State Lett. 12 (2009) A215. doi:10.1149/1.3212894.

[32] J.S. Bridel, T. Azaïs, M. Morcrette, J.M. Tarascon, D. Larcher, Key parameters governing the reversibility of Si/carbon/CMC electrodes for Li-ion batteries, Chem. Mater. 22 (2010) 1229–1241. doi:10.1021/cm902688w.

[33] M. Jiao, K. Liu, Z. Shi, C. Wang, SiO_2/Carbon Composite Microspheres with Hollow Core-Shell Structure as a High-Stability Electrode for Lithium-Ion Batteries, ChemElectroChem. 4 (2017) 542–549. doi:10.1002/celc.201600658.

[34] J. Tu, Y. Yuan, P. Zhan, H. Jiao, X. Wang, H. Zhu, S. Jiao, Straightforward Approach toward SiO_2 Nanospheres and Their Superior Lithium Storage Performance, J. Phys. Chem. C. 118 (2014) 7357–7362. doi:10.1021/jp5011023.

[35] M. Li, Y. Zeng, Y. Ren, C. Zeng, J. Gu, X. Feng, H. He, Fabrication and lithium storage performance of sugar apple-shaped SiO_x@C nanocomposite spheres, J. Power Sources. 288 (2015) 53–61. doi:10.1016/j.jpowsour.2015.04.127.

[36] Y. Yao, J. Zhang, L. Xue, T. Huang, A. Yu, Carbon-coated SiO_2 nanoparticles as anode material for lithium ion batteries, J. Power Sources. 196 (2011) 10240–10243. doi:10.1016/j.jpowsour.2011.08.009.

[37] S. Hao, Z. Wang, L. Chen, Amorphous SiO_2 in tunnel-structured mesoporous carbon and its anode performance in Li-ion batteries, Mater. Des. 111 (2016) 616–621. doi:10.1016/j.matdes.2016.09.020.

[38] A. Ostadhossein, S.Y. Kim, E.D. Cubuk, Y. Qi, A.C.T. Van Duin, Atomic Insight into the Lithium Storage and Diffusion Mechanism of SiO_2/Al_2O_3 Electrodes of Lithium

Ion Batteries: ReaxFF Reactive Force Field Modeling, J. Phys. Chem. A. 120 (2016) 2114–2127. doi:10.1021/acs.jpca.5b11908.

[39] R.S. Mulliken, Electronic Population Analysis on LCAO–MO Molecular Wave Functions. I, J. Chem. Phys. 23 (1955) 1833–1840. doi:10.1063/1.1740588.

[40] D.M. Knotter, Etching mechanism of vitreous silicon dioxide in HF-based solutions, J. Am. Chem. Soc. 122 (2000) 4345–4351. doi:10.1021/ja993803z.

7. <u>Figures and Tables captions notes</u>

Figure 1. Internal vibrational energies (a) and vibrational entropy (b) vs. temperature for the different reactions involved in the electrochemical reduction of SiO_2.

Figure 2. Free Helmholtz energy (a) and potential of lithiation (b) vs. temperature for the different products formed in the electrochemical reduction of SiO_2.

Figure 3. Phonon density of states (a) and electronic density of states (b) of the different products formed in the lithiation of SiO_2

Table I. Crystallographic parameters of the optimized CG calculation for the reactants and products of reactions 1-4.

Table II. Theoretical capacities, enthalpy and free energies change of reactions 1-4. Last column present Mulliken population analysis of lithium in different products formed in SiO_2 lithiation.

Table III. List of lithiation potentials reported in the literature for the formation of different products, stemming from SiO_2 lithiation. Each of the potential values reported on the second column, correspond to each of the products reported on the first column.

Structure	Space Group	Cell parameters (nm,º)
Li	Im-3m	a= 0.321
SiO_2	I-42d	a=0.516 ; α=88.3, β= γ=120.8
Si	Fd-3m	a=0.548
Li_2O	Fm-3m	a=0.462
Li_4SiO_4	P-1	a=0.506, b=0.471, c=0.719; α=82.7, β=71, γ=68.4
$Li_2Si_2O_5$	Ccc2	a=0.486, b=0.589, c=0.742; α=111.6
Li_2SiO_3	Cmc21	a=0.474, b=0.542, c=0.472; α=119.8

Reaction	Theoretical Capacity/mAh g^{-1}	ΔH/eV	ΔG/eV (300 K)	Li Mulliken electronic occupation in the products
1	1109	-2.83	-2.75	0.47
2	676	-4.78	-4.58	0.22
3	693	-5.70	-5.22	0.21
4	483	-5.62	-5.03	0.24

Structure	V lithiation/formation (V)	Ref
$Li_4SiO_4 + Li_2O$	0.25 cath	12
SEI; $Li_4SiO_4 + Li_2O$	0.79 cath 0.25 cath	13
$Li_2Si_2O_5$;	1.0; 0.77 cath 1.57; 1.75 anod	14
SEI; $Li_4SiO_4+Li_2Si_2O_5$; discharge of $Li_2Si_2O_5$	0.7 cath 0.28 cath 1.2 anod	33
SEI + Li_2O; $Li_2O +Li_4SiO_4$ $Li_2Si_2O_5$	0.72 cath; Below 0.4 0.4 V- 0.6	34 35
SEI; $Li_4SiO_4 + Li_2O$	0.69 cath 0.15 cath	36
SEI; Li_4SiO_4	0.72 cath 0.32 cath	37

Table III. List of lithiation potentials reported in the literature for the formation of different products, stemming from SiO_2 lithiation. Each of the potential values reported on the second column, correspond to each of the products reported on the first column. "cath" denote cathodic and "anod" denotes anodic peaks